sustainability

MDPI

Article

Electrospun Carboxymethyl Cellulose/Polyvinyl Alcohol Nanofiber Membranes for Enhanced Metal Ion Removal

Weijian Shi, Jiawei Cai, Yuan Yang, Chao Xu, Jianwei Lu and Shuping Wu *

Research School of Polymeric Materials, School of Materials Science & Engineering, Jiangsu University, Zhenjiang 212013, China

* Correspondence: shupingwu@ujs.edu.cn

Abstract: Carboxymethyl cellulose (CMC)/polyvinyl alcohol (PVA) composite nanofiber membranes were prepared by electrostatic spinning, using CMC and PVA as raw materials and glutaraldehyde as a cross-linking agent. The structure, morphology, thermal stability, and filtration performance of CMC/PVA nanofiber membranes were characterized by advanced instrumental analysis methods such as scanning electron microscopy, Fourier transform infrared spectroscopy, thermogravimetric analysis, ultraviolet analysis, and energy spectrum analysis. The results show that the average fiber diameter decreases from 381 nm to 183 nm when the spinning voltage is 23 KV and the jet speed is 2 μL/min. The obtained fiber has the smallest particle size and the most uniform distribution. Infrared spectroscopy analysis confirms that the adsorption behavior of nanofiber membranes on Cu^{2+} and Cr^{6+} is chemical adsorption. The retention rates of CMC/PVA nanofiber membranes for Cu^{2+} and Cr^{6+} reached 97.2% and 98.8%, respectively. The adsorption capacities of Cu^{2+} and Cr^{6+} were 26.34 and 28.93 $mg \cdot g^{-1}$, respectively. The adsorption of heavy metal ions by nanofiber membranes can be explained by the pseudo-second-order kinetic mechanism of the chemisorption process and the Langmuir isotherm model.

Keywords: electrospinning; nanomaterials; carboxymethyl cellulose; water purification

Citation: Shi, W.; Cai, J.; Yang, Y.; Xu, C.; Lu, J.; Wu, S. Electrospun Carboxymethyl Cellulose/Polyvinyl Alcohol Nanofiber Membranes for Enhanced Metal Ion Removal. *Sustainability* **2023**, *15*, 11331. https://doi.org/10.3390/su151411331

Academic Editor: Luca Di Palma

Received: 9 June 2023
Revised: 18 July 2023
Accepted: 19 July 2023
Published: 20 July 2023

1. Introduction

Nowadays, heavy metal pollution in water bodies has become an increasingly serious environmental and public health problem globally [1,2]. There are two main sources of heavy metals in the environment: on the one hand, in nature, different rocks contain various heavy metal elements, and soil is differentiated from rocks, which determines the initial content of heavy metals contained in the soil. Processes such as volcanic eruptions, forest fires, wind dusting, etc. make a lot of heavy metal dust float in the air and eventually enter water bodies and soil through dust fall. On the other hand, there is human activity, which is considered to be the main cause of heavy metal pollution of water bodies [3].

There is a "toxic, carcinogenic and non-biodegradable" characteristic of heavy metals; thus, they can exist in the polluted water environment for a long time and can be accumulated in organisms through the biomagnification effect of the food chain, ultimately threatening human health [4,5]. Every year, millions of people die from diseases caused by drinking contaminated water. Therefore, how to efficiently remove heavy metal ions from water bodies is an essential problem to be solved in the field of environmental protection. To date, many techniques have been used to remove heavy metal ions from wastewater, including chemical precipitation [6], membrane separation [7], ion exchange [8], and adsorption [9]. In recent decades, adsorption membrane filtration technology has become one of the most popular research hotspots. Compared with the traditional adsorption method, it has the characteristics of high efficiency, energy savings, simple operation, modularization, molecular filtration, and good effluent quality [10,11]. Accordingly, it is widely used in food, pharmaceutical, biological, chemical, energy, and water treatment fields [12,13].

At present, electrospinning technology is one of the most simple and effective methods to prepare micro- and nanofiber membranes [14–16]. The diameter of the prepared nanofibers can be adjusted from tens of nanometers to several microns [17,18]. Because of their high surface area, high removal efficiency, and high porosity, electrostatic spinning fibers are widely used in water purification fields such as oil–water separation, heavy metal ion removal, and dye removal [19,20]. In addition, electrostatically spun nanofibers can introduce various coordination and chelating groups through surface functionalization, which can easily be separated from wastewater after the adsorption of heavy metal ions, effectively reducing wastewater treatment costs and preventing the occurrence of secondary pollution [21–23].

Yang et al. prepared chitosan (CS) nanofiber membranes by electrospinning, and then successfully prepared an amine-rich CS-PGMA-polyvinylimide (PEI) electrospinning membrane by grafting PEI in a two-step method, which was used to remove heavy metal ions from an aqueous solution [24]. The filtration mechanism was analyzed by XPS. The adsorption process is divided into two parts: one is that negatively charged Cr (VI) ($HCrO^{4-}$ and Cr_2O^{7-}) is first adsorbed by protonated amino groups; second, Cr (VI) is reduced to Cr (III) by proton consumption and bonded with CS-PGMA-PEI electrospinning film. The membrane has excellent adsorption and filtration performance and stability, and the maximum adsorption capacities of Cr (VI), Cu (II), and Co (II) reach 138.96, 69.27, and 68.31 mg/g, respectively. Multi-walled carbon nanotubes (MWCNTs) and electrospinning nanofibers are ideal nanomaterials with great potential in the field of heavy metal ion removal.

Deng et al. modified MWCNTs with PEI and then prepared nanofiber membranes by electrospinning embedded polyacrylonitrile (PAN) for the removal of heavy metal ions [25]. Compared with pure PAN membranes, MWCNTs/PEI/PAN composite nanofiber membranes have higher mechanical strength, hydrophilicity, permeability, and filtration efficiency. The adsorption process is in line with chemisorption. PEI provides additional active sites for composite nanofiber membranes, which makes the adsorption capacity of Pb^{2+} and Cu^{2+} ions on composite nanofiber membranes higher than other nanocomposite membranes.

CMC is an important cellulose made from natural cellulose by carboxymethylation [26]. Its structure is rich in hydroxyl (–OH) and carboxyl (–COOH), which have strong complexation abilities with heavy metal ions in water (such as cadmium, copper, and lead) [27]. CMC has the advantages of content abundance, environmental friendliness, biodegradability, low cost, and strong adsorption capacity, and has broad application prospects in the field of heavy metal adsorption and separation [28,29]. Nevertheless, the presence of a large number of hydrogen bonds in the molecular structure of CMC and its high crystallinity makes it difficult to dissolve in common organic solvents, and it is difficult to prepare CMC fiber membranes using electrostatic spinning. Although microfibers can be obtained by electrostatic spinning of aqueous CMC solutions with a certain viscosity, these microfibers have problems such as strong water absorption, poor mechanical properties, and poor moisture resistance, which limit their application [14,30,31]. Therefore, in order to prepare excellent electrospinning nanofiber membranes and improve the stability of CMC nanofiber membranes in the process of water purification, physical and chemical modification of CMC is required [32,33].

Typically, other polymers such as polyvinylpyrrolidone (PVP), polyvinyl alcohol (PVA), and polyethylene glycol (PEG) are added to CMC to improve its mechanical strength and electrospinning processing properties. PVA is an environmentally friendly polymer of interest for its water solubility, biodegradability, biocompatibility, chemical stability, processability, and excellent spin ability [34–37]. The hydroxyl group on the PVA interacts with intermolecular and intramolecular hydrogen bonds. Due to hydrogen bonding, CMC and PVA have strong interactions together. Both polymers have excellent water solubility, which makes them tend to form homogeneous solutions [38]. Hashmi et al. blended CMC and PVA through electrostatic spinning to prepare a nanofiber film with uniform fiber

morphology, which overcame the disadvantage that CMC was too viscous to form silk [39]. Compared with pure PVA nanofiber membranes, PVA/CMC nanofibers have higher tensile strength and lower tensile strain, which greatly increases the service life and stability of CMC/PVA nanofiber membranes in extreme environments. Duran-Guerrero et al. prepared nanofiber membranes with different SMON-loading capacities using magnetic nanoparticles (SMON) loaded CMC/PVA blends as the carrier by electrospinning [40]. With the increase in SMON content, the diameter of nanofibers becomes finer and more uniform, which is mainly because SMON reduces the interaction between CMC and PVA and increases spinnability.

In this study, 2 wt% CMC aqueous solution and 5 wt% PVA aqueous solution were mixed at a mass ratio of 1:10, then 1 wt% glutaraldehyde was added to obtain a homogeneous spinning solution, and CMC/PVA nanofiber membranes were prepared by the electrostatic spinning method. The structural morphology, thermal stability, hydrophilicity, and filtration and adsorption properties of the CMC/PVA nanofiber membranes were analyzed using SEM, FT-IR, TG, WCA, UV, and EDS characterization methods. The effects of electrostatic spinning voltage on the morphology and diameter of the nanofiber membranes were investigated, and the adsorption properties of CMC/PVA nanofiber membranes on Cu^{2+} and Cr^{6+} were discussed. The prepared CMC/PVA nanofiber membranes exhibited ultra-high permeate flux and heavy metal ion removal performance.

The innovation of this study is the preparation of nanofiber membranes from CMC and PVA for the removal and filtration of heavy metal ions using electrostatic spinning technology. CMC, as a natural polymeric material, plays a key role in the preparation of nanofibrous membranes. With the advantages of hydrophilicity, biodegradability, and biocompatibility, CMC can effectively improve the surface hydrophilicity of nanofiber membranes and increase their permeation flux. CMC/PVA nanofiber membranes are prepared without the use of toxic and hazardous solvents, which is in line with the concept of green chemistry and has good prospects for application in the field of sustainable water purification membranes.

2. Experimental Section

2.1. Reagents and Instruments

The chemical reagents used in this experiment were all chemically pure, mainly including carboxymethyl cellulose (CMC), polyvinyl alcohol (PVA), copper chloride ($CuCl_2$), potassium dichromate ($K_2Cr_2O_7$), sodium diethyl dithiocarbamate, diphenylcarbodihydrazide, and anhydrous ethanol hydrochloric acid, all purchased from Sinopharm Chemical Reagent Co.

2.2. Preparation of CMC/PVA Nanofiber Membranes

First, 5 g of PVA was dissolved in 95 g of deionized water and stirred in a water bath at 90 °C for 6 h to obtain 5 wt% PVA solution. Then, 2 g of CMC was dissolved in 98 g deionized water and stirred at room temperature and high speed for 3 h to obtain a 2 wt% CMC solution. A 5 wt% PVA solution and a 2 wt% CMC solution were prepared as a 10:1 mass ratio mixed solution, and 1 wt% glutaraldehyde was added ultrasonically for 30 min, to obtain a mixed spinning solution. Finally, the mixed PVA/CMC solution was injected into the syringe, and the injection propulsion speed was controlled by the automatic propulsion device. The electrostatic voltage of the device is 17~23 kV, the receiving distance is 10 cm, and the propulsion speed is 2 μL/min.

2.3. Characterization of CMC/PVA Nanofiber Membranes

Field emission scanning electron microscopy (SEM, FEI Nova Nano 450, Hillsboro, OR, USA) was used to analyze the structure and surface morphology of nanofiber films, and the fiber thickness and distribution were analyzed by ImageJ software. The thermal stability of nanofiber membranes was analyzed by a comprehensive thermal analyzer (TG, NETZSCH STA 449 F3, Bavaria, Germany). The nanofiber films were characterized

by Fourier transform infrared absorption spectrometer (FTIR, Thermo Fisher Scientific, Nicolet iS10, MA, USA) in the wavelength range of 4000–500 cm^{-1}. An energy dispersion spectrometer (EDS, Amptek EDAX, Octane Plus, CA, USA) was used to analyze the surface elements of metal ion solutions before and after nano-fiber membrane filtration.

2.4. Preparation and UV Analysis of Cu Reagent and Cr Reagent

The Cu reagent was obtained by dissolving DDTc-Na in deionized water and preparing a 50 mg/L aqueous solution. $CuCl_2$ was dissolved in Cu reagent and 10 groups of solutions with different concentrations of Cu ions were prepared. Cu^{2+} appears yellow after reaction with Cu reagent, and the characteristic peak absorption intensity was measured at 450 nm.

The Cr reagent was prepared by adding diphenylcarbodihydrazine and 1 mmol HCl to anhydrous ethanol to form a 50 mg/L diphenylcarbodihydrazine/ethanol solution. Ten sets of solutions of different concentrations of Cr ions were prepared by dissolving $K_2Cr_2O_7$ in Cr reagent. Cr^{6+} reacted with Cr reagent to give a purple color and the intensity of its characteristic absorption peak was measured at 550 nm in the UV spectrum.

2.5. Filtration Tests of CMC/PVA Nanofiber Membranes

The separation performance of nanofiber membranes was tested by a vacuum filter device and a sand core filter device. A 0.1 g sample was taken and fixed on a sand core filter device with a diameter of 4 cm. Prior to the test, the nanofiber membranes were pretreated with deionized water at a pressure of 1 bar for 0.5 h to stabilize its water flux. To determine the retention rate of nanofiber membranes, the feed solution was prepared by dissolving $CuCl_2$ and $K_2Cr_2O_7$ in DI water with concentrations of 1 mg·L^{-1}, 5 mg·L^{-1}, and 10 mg·L^{-1}, respectively, and then filtering under 1 bar using CMC/PVA nanofiber membranes. After filtration, the concentration of Cu^{2+} and Cr^{6+} in the filtrate was determined by a UV–visible spectrophotometer (UV, Shimadzu, UV-2700, Kyoto, Japan). All filtration experiments were performed at room temperature. The water flux (J, L m^{-2} h^{-1} bar^{-1}) and rejection (R) were calculated by the following Equations (1) and (2), respectively.

$$J = \frac{\mathrm{A}}{VP\Delta t} \tag{1}$$

$$R = \frac{C_f - C_p}{C_f} \times 100\% \tag{2}$$

where V (L) is the volume of permeated water over a time interval Δt (h); A (m^2) is the area of the membrane; P (bar) is the operating pressure; C_f is the concentration of feed solution and C_p is the concentration of permeate solution.

2.6. Adsorption Study of CMC/PVA Nanofiber Membranes

The adsorption performance of the CMC/PVA nanofiber membranes was assessed by adding 0.1 g of the obtained membranes to $CuCl_2$ and $K_2Cr_2O_7$ solutions, respectively, at an initial concentration of 30 mg·L^{-1} for 100 mL. The concentration of metal ions in the solutions was determined by UV–vis at room temperature. The amount of adsorption was assessed by using the following expressions:

$$q_t = \frac{C_0 - C_t}{\mathrm{m}} \times V \tag{3}$$

$$q_e = \frac{C_0 - C_e}{\mathrm{m}} \times V \tag{4}$$

where C_0 and C_e (mg·L^{-1}) are the initial concentration and equilibrium concentration of the heavy metal ion solution, q_t (mg·L^{-1}) and C_t (mg·L^{-1}) are the adsorption capacity and concentration of CMC nanofiber membrane at time, q_e (mg·L^{-1}) is the equilibrium

adsorption capacity, V (L) is the volume of the heavy metal ion solution and m (g) is the mass of CMC nanofiber membrane.

3. Results and Discussion

3.1. Characteristics of Nanofiber Membranes

Figure 1 describes the preparation strategy and filtration principle of the CMC/PVA nanofiber membrane. A CMC/PVA homogeneous spinning solution was prepared by mixing CMC and PVA in proportion into the syringe, which was connected to the high-voltage power supply, and then the drum receiving device was connected to the ground wire. Finally, a CMC/PVA nanofiber membrane was prepared by electrospinning. Through the filtration and adsorption characteristics of the nanofiber membrane, it was used for environmental water purification. However, voltage is related to the stability of the Taylor cone and is one of the decisive factors affecting the morphology of electrostatically spun nanofibers [41,42]. Therefore, we prepared CMC/PVA nanofiber membranes under different voltage conditions. Figure 2 shows the SEM image and diameter distribution of CMC/PVA nanofiber films at different spinning voltages. As can be seen from Figure 2, when the voltage is 17 KV, the nanofibers show an obvious beading phenomenon. When the voltage was increased to 23 KV, the bead string phenomenon disappeared, and the distribution of the prepared nanofibers was the most uniform. It is speculated that the coulomb force is increased by increasing the voltage, which makes the mixed solution diverge directly into the fiber structure.

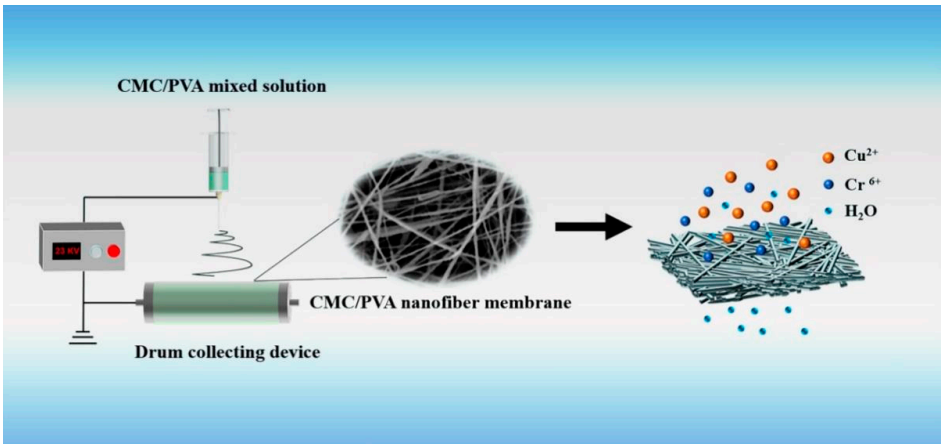

Figure 1. Schematic illustration for the preparation of CMC/PVA nanofiber membranes.

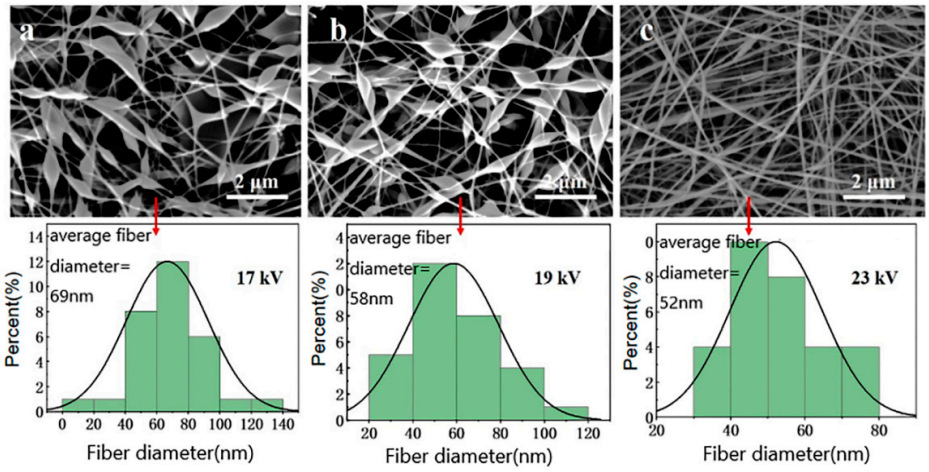

Figure 2. Surface morphology and direct distribution of CMC/PVA nanofiber membranes under different spinning voltage conditions: (**a**) 17 kV; (**b**) 19 kV; (**c**) 23 kV.

The diameter distribution of CMC/PVA nanofibers is shown in Figure 2. It can be seen that the electrostatic voltage has a great influence on the fiber diameter of the CMC/PVA nanofiber membrane. The diameter of CMC/PVA nanofibers decreases with an increase in electrostatic voltage. When the electrostatic voltage was 17 kV, the diameter of the nanofibers ranged from 0–140 nm, with an average of 69 nm. When the voltage was 23 kV, the diameter of the nanofibers mainly ranged from 30 nm to 80 nm, with an average of 52 nm. This was mainly due to the increased electrostatic field effect and the enhanced Coulomb force caused by the increased electrostatic voltage, which increased the degree of tearing of the fibers. At 23 kV, the CMC/PVA nanofibers have the smallest volume, resulting in the highest density, which greatly increases the effective filtration area and facilitates the interception of contaminants in the water.

The CMC/PVA nanofiber membrane with the best morphology was chosen as the sample for the water contact angle test, and the results of the contact angle and droplet diameter changes with time are shown in Figure 3. After the water droplet touched the membrane surface, it penetrated downward rapidly, the contact angle decreased rapidly, and the diameter increased with its decrease. After 1 s, the changes in both tended to level off. At around 2 s, the droplet diameter stopped changing, and the contact angle finally stabilized at 11.3°. The results show that the CMC/PVA nanofiber membrane has good hydrophilicity and should theoretically have high permeability, which is a very ideal substrate material for water purification membranes.

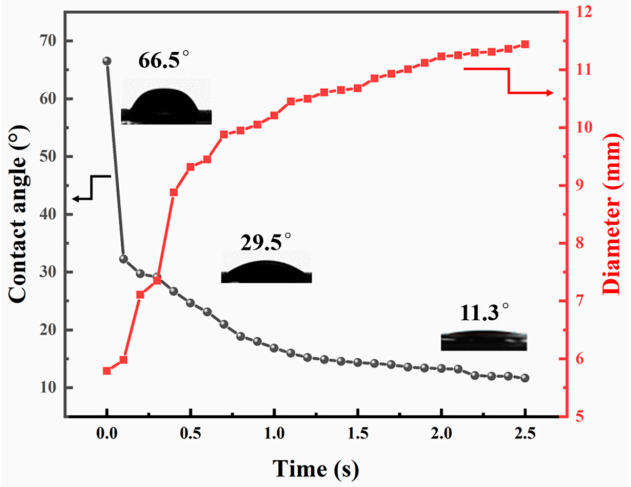

Figure 3. Trend of water contact angle (circle, gray) and droplet diameter (square, red) of CMC/PVA nanofiber membranes with time.

The thermal stability of the CMC/PVA nanofiber membrane, CMC and PVA was tested by TG and the results are shown in Figure 4. It can be seen that the pyrolysis process of the CMC/PVA nanofiber membrane, CMC and PVA was divided into four main stages. In the first stage, from 54.87 °C to 182.3 °C, the CMC/PVA nanofiber membrane was able to remain stable with essentially no change in mass. In the second stage, the water of crystallization in the samples gradually evaporated between 52.3 °C and 223.3 °C and all three started to lose weight slowly. The weight loss rates of CMC/PVA nanofiber membrane, CMC and PVA were 10%, 10%, and 8%, respectively. In the third stage, from 223.3 °C to 288.8 °C, thermal decomposition temperatures of 263.3 °C, 248.3 °C, and 252.3 °C can be seen for CMC/PVA nanofiber films, CMC and PVA, respectively, with weight loss rates reaching maximum values at 288.8 °C, 289.8 °C, and 263.3 °C. At 321.3 °C, 321.3 °C, and 309.8 °C, the weight loss rate slowed down, and the mass residuals were 36.8%, 36.3%, and 53.5% for all three, respectively. This stage is the main stage of thermal decomposition of the sample, where long-chain molecules gradually break down into smaller molecules and vaporize, resulting in significant weight loss. The fourth stage is the carbonization stage, where the remaining final residue is further decomposed to form carbon and ash.

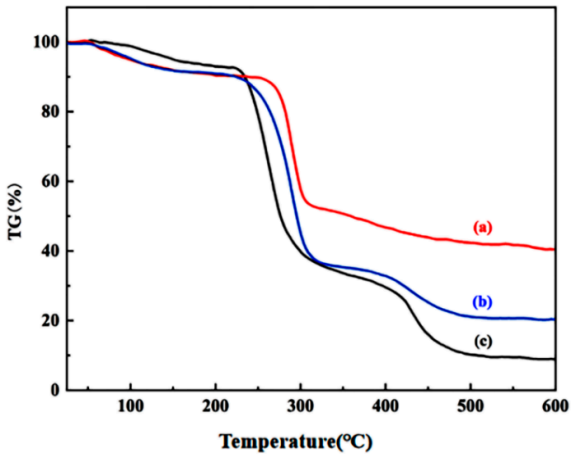

Figure 4. TG curves: (a) CMC, (b) CMC/PVA nanofiber membranes, and (c) PVA.

The changes in functional groups of CMC/PVA nanofiber membranes before and after filtration were investigated by infrared spectroscopy. As shown in Figure 5, for the CMC/PVA nanofiber membranes before filtration, the peak at 3441 cm^{-1} corresponds to the N-H stretching vibration, the peak at 1635 cm^{-1} corresponds to the bending vibration of the amide I band, the peak at 1319 cm^{-1} corresponds to the C-N stretching vibration of the amide III band, the peak at 3441 cm^{-1} corresponds to the O-H stretching vibration of the intermolecular hydrogen bond. The measurements 2920 cm^{-1} and 1031 cm^{-1} correspond to the absorption peaks of the C-H and C-O stretching vibrations, respectively. The measurement 1319 cm^{-1} corresponds to the carbonyl C-O stretching vibration absorption peak, while the CMC/PVA nanofiber membrane contains a large amount of carbonyl groups, which can be clearly seen from the CMC/PVA nanofiber membrane before and after filtration and adsorption. After the carbonyl groups are combined with Cu^{2+} and Cr^{6+} in the adsorption and filtration, the carbonyl groups. The infrared absorption peak of the CMC/PVA nanofiber membrane is weakened. This indicates that heavy metal ions in CMC/PVA nanofiber membranes undergo coordination reactions with intermolecular hydrogen bonds and carbonyl groups, which chelate with cations to form complexes, enhancing the removal of heavy metal ions by CMC/PVA nanofiber membranes. This also reflects the interaction between CMC/PVA nanofiber membranes and heavy metal ions as chemisorption.

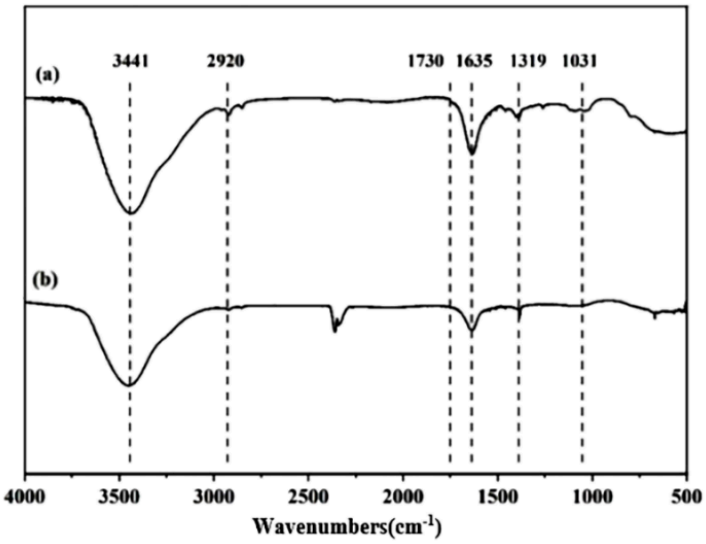

Figure 5. FT-IR spectra of CMC/PVA nanofiber membranes before and after filtration of heavy metal ions: (a) CMC/PVA fiber membrane before filtration, (b) CMC/PVA fiber membrane after filtration.

Figure 6 shows the EDS spectra of the surface elemental analysis of the nanofiber membranes before and after filtration. The presence of Cu and Cr on the surface of the CMC/PVA nanofiber membrane after filtration indicates that the carbonyl groups in the CMC/PVA nanofiber membrane combined with Cu^{2+} and Cr^{6+} in the filtrate to form strongly bound complexes with binding energies of 0.93 eV and 0.61 eV, respectively. During filtration, the CMC/PVA nanofiber membrane surface adsorbed heavy metal ions to form complexes, thus effectively removing them. The CMC/PVA nanofiber membranes formed complexes by adsorption of heavy metal ions on the surface during filtration, thus effectively removing heavy metal ions from wastewater.

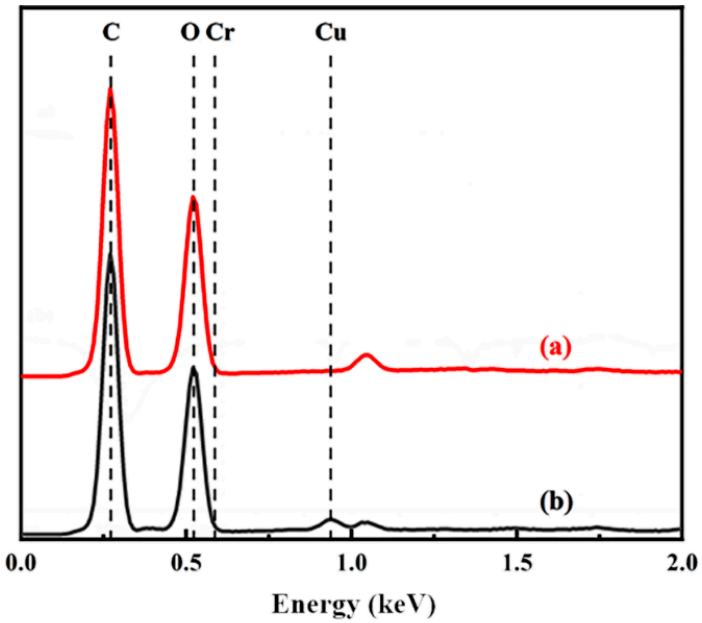

Figure 6. EDS spectra of CMC/PVA nanofiber membranes before and after filtration of heavy metal ions: (a) CMC/PVA fiber membrane before filtration, (b) CMC/PVA fiber membrane after filtration.

3.2. Adsorption Studies of the CMC/PVA Nanofiber Membranes

By performing adsorption tests on nanofiber membranes, we can help to understand the mechanism of adsorption of water contaminants by nanofiber membranes, which is crucial in practical applications. In this study, the adsorption kinetics of CMC/PVA nanofiber membranes were investigated using pseudo-first-order and pseudo-second-order kinetic models.

The pseudo-first-order kinetic model:

$$\ln(q_e - q_t) = -k_1 + \ln q_e \tag{5}$$

The pseudo-second-order kinetic model:

$$\frac{t}{q_t} = \frac{t}{q_e} + \frac{1}{k_2 q_{e^2}} \tag{6}$$

where k_1 (min^{-1}) and k_2 ($g \cdot mg^{-1} \cdot min^{-1}$) are the pseudo-first-order and pseudo-second-order rate constants, respectively.

The results of the proposed primary and proposed secondary kinetic fits are shown in Figure 7, and the corresponding kinetic parameters calculated from the above two kinetic models are shown in Table 1.

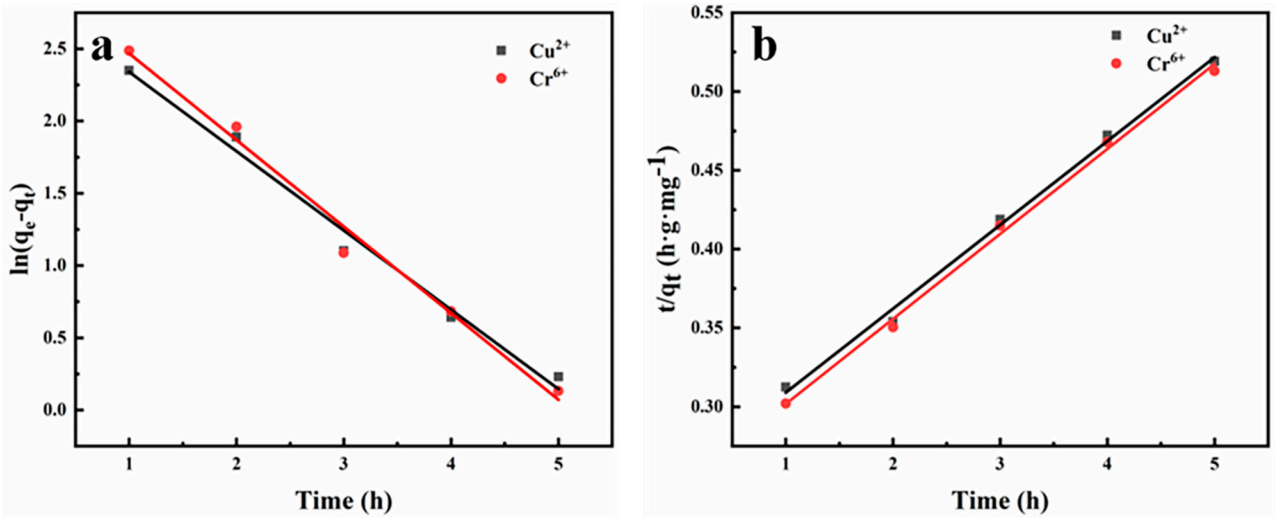

Figure 7. Kinetic models of (**a**) pseudo-first-order and (**b**) pseudo-second-order.

Table 1. Kinetic parameter for the adsorption of various pollutants on CMC/PVA.

	Nanofibrous Membrane						
		Pseudo-First-Order Model			Pseudo-Second-Order Model		
	q_{exp}	q_e	k_1	R^2	q_e	k_2 ($\times 10^{-2}$)	R^2
Cu^{2+}	15.13	17.81	0.5486	0.9869	18.80	1.10	0.9961
Cr^{6+}	16.87	19.68	0.5991	0.9875	18.53	1.18	0.9967

The adsorption processes of Cu^{2+} and Cr^{6+} fit better with the proposed secondary kinetic model (correlation coefficients R^2 of 0.9961 and 0.9967, respectively), which implies that the corresponding adsorption processes are dominated by chemisorption. The equilibrium adsorption amounts (q_e) calculated by Equations (5) and (6) were also closer to the experimentally measured equilibrium adsorption amounts (q_{exp}).

The interaction of target contaminants with nanofiber membranes was evaluated using adsorption isotherms (i.e., Langmuir and Freundlich models).

Langmuir adsorption isotherm model is expressed as equation:

$$\frac{C_e}{q_e} = \frac{C_e}{q_{max}} + \frac{1}{k_L q_{max}} \quad (7)$$

$$lnq_e = \frac{1}{n} lnC_e + lnK_F \quad (8)$$

where C_e (mg·L^{-1}) is the equilibrium concentration of heavy metal ion solution, q_e (mg·g^{-1}) is the equilibrium adsorption capacity of heavy metal ion adsorbed on CMC nanofiber film, q_{max} (mg·g^{-1}) is the maximum adsorption capacity of CMC nanofiber membrane, and K_L (L·mg^{-1}) is the Langmuir adsorption equilibrium constant. K_F (mg·g^{-1}) is the Freundlich constant and n is the adsorption strength correlation constant.

In addition, the thermodynamic isotherms are shown in Figure 8, and the corresponding linear fits allow the relevant equilibrium coefficients to be obtained, the results of which are shown in Table 2. The adsorption processes of Cu^{2+} and Cr^{6+} fit well with the Langmuir model (correlation coefficients R^2 of 0.9994 and 0.9989, respectively), indicating that the adsorption process was dominated by monolayer adsorption, and the maximum adsorption amounts of Cu^{2+} and Cr^{6+} were 26.34 and 28.93 mg·g^{-1}, respectively. In the Freundlich model, the magnitude of the KF value represents the corresponding adsorption capacity intensity, and the trend of this value is also in good agreement with the corresponding q_{max}.

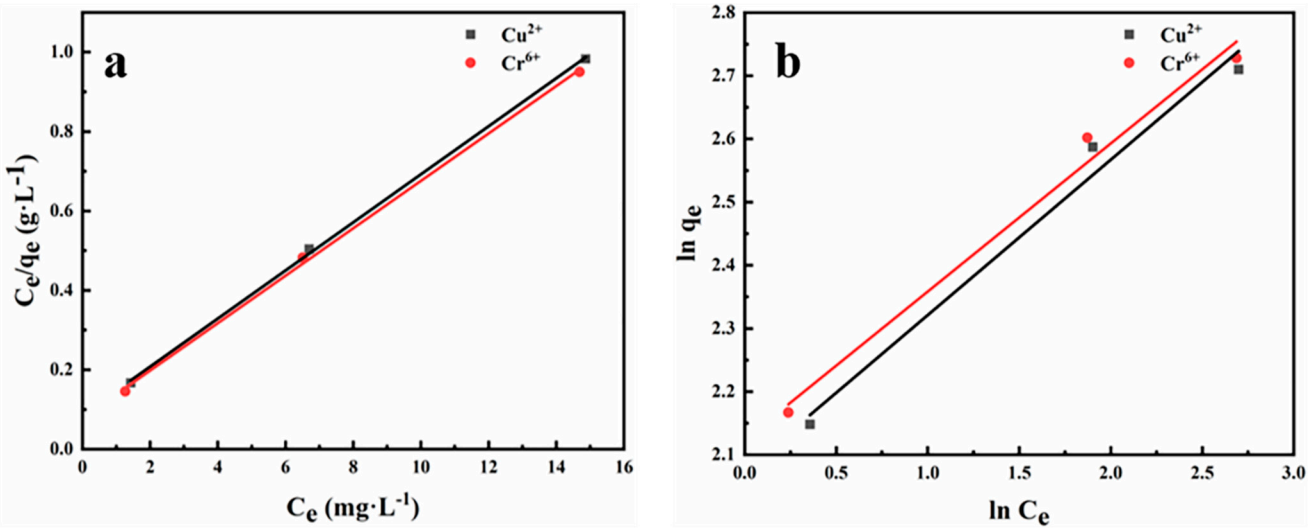

Figure 8. Adsorption isotherms: (**a**) Langmuir and (**b**) Freundlich.

Table 2. Isotherm parameters for the adsorption of various pollutants on CMC/PVA.

	Nanofibrous Membrane					
	Langmuir Isotherm Model			Freundlich Isotherm Model		
	q_{max}	K_L	R^2	n	K_F	R^2
Cu^{2+}	26.34	0.4364	0.9994	4.06	7.965	0.9828
Cr^{6+}	28.93	0.4381	0.9989	4.26	8.364	0.9864

The K_L of the nanofiber membrane for Cu^{2+} and Cr^{6+} was calculated by the Langmuir isotherm model to be 0.4364 and 0.4381, respectively, indicating that Cu^{2+} and Cr^{6+} bind well to the nanofiber membrane. In conclusion, this nanofiber membrane has good filtration and adsorption properties due to its uniform pore size, good permeability, and the physicochemical interaction between the carbonyl and hydroxyl groups on the nanofibers and the contaminants.

3.3. Nanofiber Membranes Flux and Separation Performance

Figure 9a shows the UV absorption curves of 10 sets of Cu^{2+} solutions (concentrations of 0.55, 0.60, 0.65, 0.70, 0.75, 0.80, 0.85, 0.90, 0.95, and 1.00 mg/L, respectively). The corresponding standard curves were obtained by linear fitting with origin software (Figure 9b) with a linear correlation coefficient (R^2) of 0.9966. The maximum absorption peak was substituted into the equation obtained by linear fitting, and the Cu^{2+} solution concentrations before and after filtration were calculated, and then the Cu^{2+} concentrations before and after filtration were substituted into Equation (2). The final CMC/PVA nanofiber membranes obtained showed good adsorption and filtration of 1 mg·L^{-1}, 5 mg·L^{-1}, and 10 mg·L^{-1} Cu^{2+} with retention rates of 97.2%, 93.11%, and 92.94%, respectively (Figure 9c).

Figure 10a shows the UV absorption curves of 10 sets of Cr^{6+} solutions (concentrations of 0.55, 0.60, 0.65, 0.70, 0.75, 0.80, 0.85, 0.90, 0.95, and 1.00 mg·L^{-1}, respectively), measured in UV–vis. Origin software was linearly fitted to obtain the corresponding standard curves (Figure 10b) with a linear correlation coefficient (R^2) of 0.9944. The maximum absorption peak was substituted into the equation obtained by linear fitting, and the Cr^{6+} solution concentrations before and after filtration were calculated, and then the Cr^{6+} concentrations before and after filtration were substituted into Equation (2). The final CMC/PVA nanofiber membranes obtained showed good adsorption and filtration of 1 mg·L^{-1}, 5 mg·L^{-1}, and 10 mg·L^{-1} Cr^{6+} with retention rates of 98.8%, 96.12%, and 94.67%, respectively (Figure 10c).

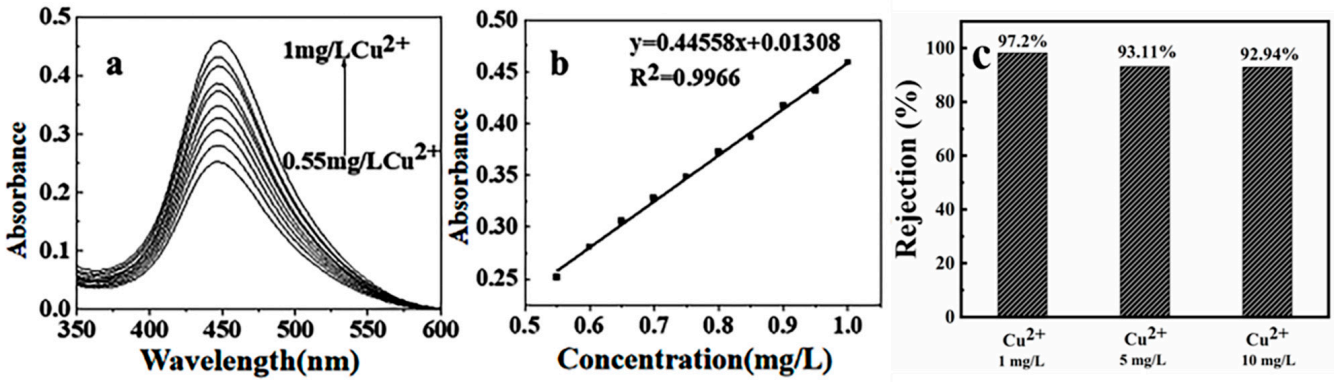

Figure 9. (**a**) UV absorption curves of Cu^{2+} at different concentrations, (**b**) standard curve of Cu^{2+} UV absorption peak, (**c**) rejection rates of 1 mg·L^{-1}, 5 mg·L^{-1}, and 10 mg·L^{-1} Cu2+ by CMC/PVA nanofiber membranes.

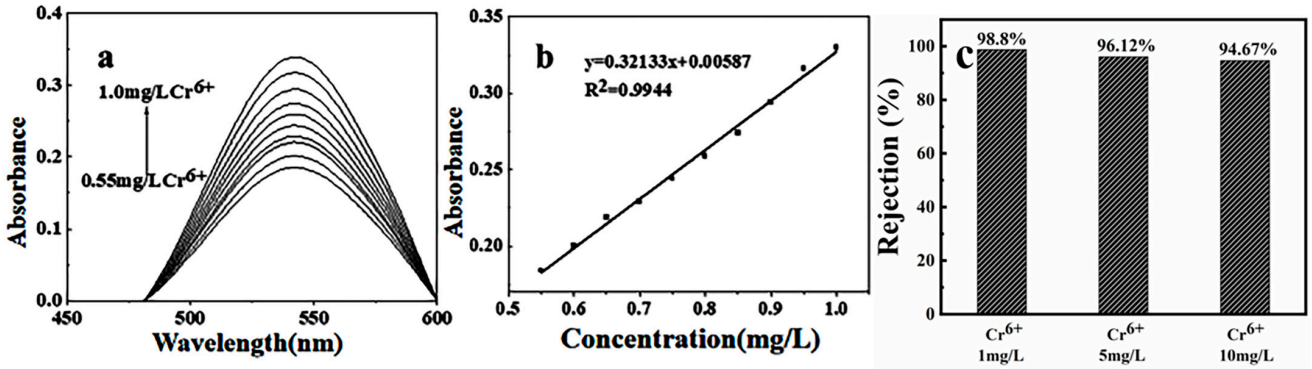

Figure 10. (**a**) UV absorption curves of Cr^{6+} at different concentrations, (**b**) standard curve of Cr^{6+} UV absorption peak, (**c**) rejection rates of 1 mg·L^{-1}, 5 mg·L^{-1}, and 10 mg·L^{-1} Cr^{6+} by CMC/PVA nanofiber membranes.

The permeate fluxes of the CMC/PVA nanofiber membranes to pure water and each target contaminant solution were calculated separately according to Equation (1), and the concentrations of metal ions in the filtrate were detected using UV–vis, the results of which are shown in Figure 11. The CMC/PVA nanofiber membranes can achieve a pure water flux of 4398 L·m^{-2}·h^{-1}, which is higher than the general ultrafiltration membrane; the permeate fluxes of 1 mg·L^{-1}, 5 mg·L^{-1}, 10 mg·L^{-1} Cu^{2+}, 1 mg·L^{-1}, 5 mg·L^{-1}, and 10 mg·L^{-1} Cr^{6+} can reach 4083, 4050, 3931, 3862, 3747, 3721 L·m^{-2}·h^{-1}, respectively.

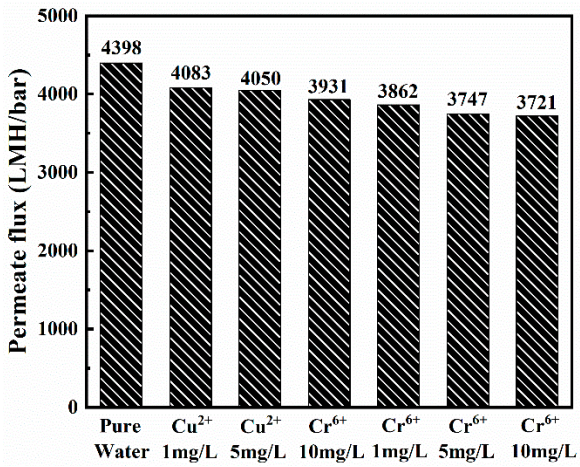

Figure 11. Permeate flux of Cu^{2+} and Cr^{6+} with CMC/PVA nanofiber membranes.

The recyclability of CMC/PVA nanofiber membranes was tested with 100 mL of 10 mg·L^{-1} Cu^{2+} and Cr^{6+}. Each filtration interval was one hour and a total of five tests were carried out with the results shown in Figure 12. There was no significant decrease in permeate flux and filtration performance after five filtration cycles. This indicates that the nanofiber membranes have good recyclability and can be used for a long time.

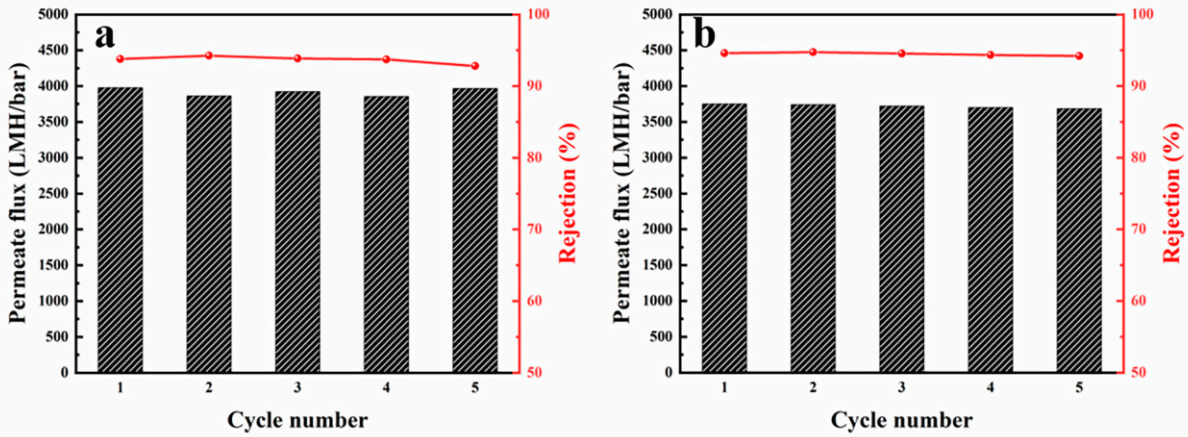

Figure 12. Cycle testing of CMC/PVA nanofiber membranes (**a**) Cu^{2+} and (**b**) Cr^{6+}.

In summary, when the prepared CMC/PVA nanofiber membranes were compared with other natural polymeric filtration membranes, the CMC/PVA nanofiber membranes had significantly higher permeate flow rates and good heavy metal removal efficiencies (as shown in Table 3). Although the filtration efficiency was slightly lower than that of the GO/gravitate/Al_2O_3 composite membrane, the CMC/PVA nanofiber membranes prepared in this study were green, non-polluting, and environmentally friendly, in line with the sustainable development strategy. The permeate flux is directly related to the porosity, pore size, and hydrophilicity of the membrane surface. In this paper, CMC/PVA nanofiber membranes with high porosity, high permeability, and high hydrophilicity were successfully prepared by controlling the electrostatic spinning process parameters using the hydrophilic and co-spinning properties of PVA.

Table 3. Comparison of adsorption performance by some nanofiber membranes.

Membrane Type	Heavy Metal Ion	Rejection Rate	Reference
GO/Attapulgite/Al_2O_3	Cu^{2+}	99.9%	[43]
PVA/IC/PANI/GO	Pb^{2+}, Cd^{2+}	97.19%, 91.4%	[44]
PVC/TNT	Cu^{2+}, Ni^{2+}	90%, 86.7%	[45]
PU/ZIF	Cr^{6+}	85%	[46]
PEI/TMC	Zn^{2+}, Cd^{2+}, Ni^{2+}, Cu^{2+}	97%	[47]
PVDF/α-ZrP	Cu^{2+}, Pb^{2+}	93.1%, 91.2%	[48]
CA/P(MA-co-AA)/PEI	Cu^{2+}	97.4%	[49]
CS/Fe_3O_4@SiO_2	Cu^{2+}, Pb^{2+}	98.61%, 98.11%	[50]
CMC/PVA	Cu^{2+}, Cr^{2+}	97.2%, 98.8%	This work

4. Conclusions

CMC/PVA nanofiber membranes for adsorption and filtration of heavy metal ions in aqueous solutions were synthesized by the electrostatic spinning technique and characterized by SEM, FTIR, WCA, and TG. GA vapor could well promote the cross-linking of nanofibers and increase the effective adsorption area of nanofiber membranes. The maximum monolayer adsorption amounts of Cu (II) and Cr (VI) were 26.34 and 28.93 mg·g^{-1}, respectively. The adsorption isotherms of heavy metal ions on the CMC/PVA nanofiber membranes were in accordance with the Langmuir model and the adsorption kinetics were in accordance with the fitted second-order model. In addition, the CMC/PVA nanofiber

membranes showed good separation performance with a permeation capacity of up to 4398 $L \cdot m^{-2} \cdot h^{-1} \cdot bar^{-1}$ for pure water and retention rates of 97.2% and 98.8% for Cu (II) and Cr (VI), respectively. Thus, CMC/PVA nanofiber membranes are expected to be the ideal material for a new generation of sustainable water purification membranes due to their good adsorption and separation of heavy metal ions, and their environmental friendliness and spontaneous degradation.

Author Contributions: Conceptualization, J.L. and J.C.; methodology, C.X.; validation, W.S. and J.C.; formal analysis, W.S. and Y.Y; investigation, W.S. and S.W.; writing—original draft preparation, W.S. and Y.Y.; writing—review and editing, S.W.; visualization, W.S. and J.C.; supervision, S.W.; project administration, S.W.; funding acquisition, S.W. All authors have read and agreed to the published version of the manuscript.

Funding: This work was supported by the National Natural Science Foundation of China (51808263) and the Youth Talent Cultivation Program of Jiangsu University (2018).

Institutional Review Board Statement: Not applicable.

Informed Consent Statement: Not applicable.

Data Availability Statement: Not applicable.

Conflicts of Interest: The authors declare no conflict of interest.

References

1. Mishra, S.; Bharagava, R.N.; More, N.; Yadav, A.; Zainith, S.; Mani, S.; Chowdhary, P. Heavy metal contamination: An alarming threat to environment and human health. In *Environmental Biotechnology: For Sustainable Future*; Springer: Singapore, 2018; pp. 103–125.
2. Han, R.; Zhou, B.; Huang, Y.; Lu, X.; Li, S.; Li, N. Bibliometric overview of research trends on heavy metal health risks and impacts in 1989–2018. *J. Clean. Prod.* **2020**, *276*, 123249. [CrossRef]
3. Kapoor, D.; Singh, M.P. Heavy metal contamination in water and its possible sources. In *Heavy Metals in the Environment*; Elsevier: Amsterdam, The Netherlands, 2021; pp. 179–189.
4. Ali, H.; Khan, E.; Ilahi, I. Environmental chemistry and ecotoxicology of hazardous heavy metals: Environmental persistence, toxicity, and bioaccumulation. *J. Chem.* **2019**, *2019*, 6730305. [CrossRef]
5. Vardhan, K.H.; Kumar, P.S.; Panda, R.C. A review on heavy metal pollution, toxicity and remedial measures: Current trends and future perspectives. *J. Mol. Liq.* **2019**, *290*, 111197. [CrossRef]
6. Qasem, N.A.; Mohammed, R.H.; Lawal, D.U. Removal of heavy metal ions from wastewater: A comprehensive and critical review. *Npj Clean Water* **2021**, *4*, 36. [CrossRef]
7. Qi, Y.; Zhu, L.; Shen, X.; Sotto, A.; Gao, C.; Shen, J. Polythyleneimine-modified original positive charged nanofiltration membrane: Removal of heavy metal ions and dyes. *Sep. Purif. Technol.* **2019**, *222*, 117–124. [CrossRef]
8. Merino-Garcia, I.; Velizarov, S. New insights into the definition of membrane cleaning strategies to diminish the fouling impact in ion exchange membrane separation processes. *Sep. Purif. Technol.* **2021**, *277*, 119445. [CrossRef]
9. Velusamy, S.; Roy, A.; Sundaram, S.; Kumar Mallick, T. A review on heavy metal ions and containing dyes removal through graphene oxide-based adsorption strategies for textile wastewater treatment. *Chem. Rec.* **2021**, *21*, 1570–1610. [CrossRef]
10. Liang, B.; He, X.; Hou, J.; Li, L.; Tang, Z. Membrane separation in organic liquid: Technologies, achievements, and opportunities. *Adv. Mater.* **2019**, *31*, 1806090. [CrossRef]
11. Tijing, L.D.; Dizon, J.R.C.; Ibrahim, I.; Nisay, A.R.N.; Shon, H.K.; Advincula, R.C. 3D printing for membrane separation, desalination and water treatment. *Appl. Mater. Today* **2020**, *18*, 100486. [CrossRef]
12. Ni, J.; Yuan, C.; Zheng, J.; Liu, Y. Distributions, contamination level and ecological risk of heavy metals in surface sediments from intertidal zone of the Sanmen Bay, East China. *J. Sea Res.* **2022**, *190*, 102302. [CrossRef]
13. Pronk, W.; Ding, A.; Morgenroth, E.; Derlon, N.; Desmond, P.; Burkhardt, M.; Wu, B.; Fane, A.G. Gravity-driven membrane filtration for water and wastewater treatment: A review. *Water Res.* **2019**, *149*, 553–565. [CrossRef] [PubMed]
14. Liu, M.; Cai, N.; Chan, V.; Yu, F. Development and applications of MOFs derivative one-dimensional nanofibers via electrospinning: A mini-review. *Nanomaterials* **2019**, *9*, 1306. [CrossRef]
15. Cui, J.; Li, F.; Wang, Y.; Zhang, Q.; Ma, W.; Huang, C. Electrospun nanofiber membranes for wastewater treatment applications. *Sep. Purif. Technol.* **2020**, *250*, 117116. [CrossRef]
16. Wu, S.; Li, K.; Shi, W.; Cai, J. Chitosan/polyvinylpyrrolidone/polyvinyl alcohol/carbon nanotubes dual layers nanofibrous membrane constructed by electrospinning-electrospray for water purification. *Carbohydr. Polym.* **2022**, *294*, 119756. [CrossRef]
17. Sun, Y.; Cheng, S.; Lu, W.; Wang, Y.; Zhang, P.; Yao, Q. Electrospun fibers and their application in drug controlled release, biological dressings, tissue repair, and enzyme immobilization. *RSC Adv.* **2019**, *9*, 25712–25729. [CrossRef] [PubMed]

18. Wu, J.; Zhang, Z.; Zhou, W.; Liang, X.; Zhou, G.; Han, C.C.; Xu, S.; Liu, Y. Mechanism of a long-term controlled drug release system based on simple blended electrospun fibers. *J. Control. Release* **2020**, *320*, 337–346. [CrossRef]
19. Zhou, Y.; Liu, Y.; Zhang, M.; Feng, Z.; Yu, D.-G.; Wang, K. Electrospun nanofiber membranes for air filtration: A review. *Nanomaterials* **2022**, *12*, 1077. [CrossRef]
20. Farokhi, M.; Mottaghitalab, F.; Reis, R.L.; Ramakrishna, S.; Kundu, S.C. Functionalized silk fibroin nanofibers as drug carriers: Advantages and challenges. *J. Control. Release* **2020**, *321*, 324–347. [CrossRef]
21. Wu, W.; Zhang, X.; Qin, L.; Li, X.; Meng, Q.; Shen, C.; Zhang, G. Enhanced MPBR with polyvinylpyrrolidone-graphene oxide/PVDF hollow fiber membrane for efficient ammonia nitrogen wastewater treatment and high-density Chlorella cultivation. *Chem. Eng. J.* **2020**, *379*, 122368. [CrossRef]
22. Zou, P.; Lee, W.-H.; Gao, Z.; Qin, D.; Wang, Y.; Liu, J.; Sun, T.; Gao, Y. Wound dressing from polyvinyl alcohol/chitosan electrospun fiber membrane loaded with OH-CATH30 nanoparticles. *Carbohydr. Polym.* **2020**, *232*, 115786. [CrossRef]
23. Deng, Y.; Lu, T.; Cui, J.; Samal, S.K.; Xiong, R.; Huang, C. Bio-based electrospun nanofiber as building blocks for a novel eco-friendly air filtration membrane: A review. *Sep. Purif. Technol.* **2021**, *277*, 119623. [CrossRef]
24. Yang, D.; Li, L.; Chen, B.; Shi, S.; Nie, J.; Ma, G. Functionalized chitosan electrospun nanofiber membranes for heavy-metal removal. *Polymer* **2019**, *163*, 74–85. [CrossRef]
25. Deng, S.; Liu, X.; Liao, J.; Lin, H.; Liu, F. PEI modified multiwalled carbon nanotube as a novel additive in PAN nanofiber membrane for enhanced removal of heavy metal ions. *Chem. Eng. J.* **2019**, *375*, 122086. [CrossRef]
26. Rahman, M.M.; Alam, M.; Rahman, M.M.; Susan, M.A.B.H.; Shaikh, M.A.A.; Nayeem, J.; Jahan, M.S. A novel approach in increasing carboxymethylation reaction of cellulose. *Carbohydr. Polym. Technol. Appl.* **2022**, *4*, 100236. [CrossRef]
27. Hamdan, M.A.; Ramli, N.A.; Othman, N.A.; Amin, K.N.M.; Adam, F. Characterization and property investigation of microcrystalline cellulose (MCC) and carboxymethyl cellulose (CMC) filler on the carrageenan-based biocomposite film. *Mater. Today Proc.* **2021**, *42*, 56–62. [CrossRef]
28. Mohamadpour, F. Carboxymethyl cellulose (CMC) as a recyclable green catalyst promoted eco-friendly protocol for the solvent-free synthesis of 1H-pyrazolo[1, 2-b]phthalazine-5,10-dione derivatives. *Polycycl. Aromat. Compd.* **2022**, *42*, 1091–1102. [CrossRef]
29. Allafchian, A.; Hosseini, H.; Ghoreishi, S.M. Electrospinning of PVA-carboxymethyl cellulose nanofibers for flufenamic acid drug delivery. *Int. J. Biol. Macromol.* **2020**, *163*, 1780–1786. [CrossRef]
30. Shen, H.; Li, Y.; Yao, W.; Yang, S.; Yang, L.; Pan, F.; Chen, Z.; Yin, X. Solvent-free cellulose nanocrystal fluids for simultaneous enhancement of mechanical properties, thermal conductivity, moisture permeability and antibacterial properties of polylactic acid fibrous membrane. *Compos. Part B Eng.* **2021**, *222*, 109042. [CrossRef]
31. Wang, C.; Zhao, J.; Liu, L.; Zhang, P.; Wang, X.; Yu, J.; Ding, B. Transformation of fibrous membranes from opaque to transparent under mechanical pressing. *Engineering* **2022**, *19*, 84–92. [CrossRef]
32. Mazuki, N.; Majeed, A.A.; Nagao, Y.; Samsudin, A. Studies on ionics conduction properties of modification CMC-PVA based polymer blend electrolytes via impedance approach. *Polym. Test.* **2020**, *81*, 106234. [CrossRef]
33. Al-Shamari, A.; Abdelghany, A.; Alnattar, H.; Oraby, A. Structural and optical properties of PEO/CMC polymer blend modified with gold nanoparticles synthesized by laser ablation in water. *J. Mater. Res. Technol.* **2021**, *12*, 1597–1605. [CrossRef]
34. Behdarvand, F.; Valamohammadi, E.; Tofighy, M.A.; Mohammadi, T. Polyvinyl alcohol/polyethersulfone thin-film nanocomposite membranes with carbon nanomaterials incorporated in substrate for water treatment. *J. Environ. Chem. Eng.* **2021**, *9*, 104650. [CrossRef]
35. Cui, Z.; Zheng, Z.; Lin, L.; Si, J.; Wang, Q.; Peng, X.; Chen, W. Electrospinning and crosslinking of polyvinyl alcohol/chitosan composite nanofiber for transdermal drug delivery. *Adv. Polym. Technol.* **2018**, *37*, 1917–1928. [CrossRef]
36. Raksa, A.; Numpaisal, P.-o.; Ruksakulpiwat, Y. The effect of humidity during electrospinning on morphology and mechanical properties of SF/PVA nanofibers. *Mater. Today Proc.* **2021**, *47*, 3458–3461. [CrossRef]
37. Unal, B.; Yalcinkaya, E.E.; Demirkol, D.O.; Timur, S. An electrospun nanofiber matrix based on organo-clay for biosensors: PVA/PAMAM-Montmorillonite. *Appl. Surf. Sci.* **2018**, *444*, 542–551. [CrossRef]
38. Khan, M.Q.; Kharaghani, D.; Ullah, S.; Waqas, M.; Abbasi, A.M.R.; Saito, Y.; Zhu, C.; Kim, I.S. Self-cleaning properties of electrospun PVA/TiO2 and PVA/ZnO nanofibers composites. *Nanomaterials* **2018**, *8*, 644. [CrossRef]
39. Hashmi, M.; Ullah, S.; Ullah, A.; Saito, Y.; Haider, M.K.; Bie, X.; Wada, K.; Kim, I.S. Carboxymethyl Cellulose (CMC) Based Electrospun Composite Nanofiber Mats for Food Packaging. *Polym.* **2021**, *13*, 302. [CrossRef]
40. Duran-Guerrero, J.G.; Martinez-Rodriguez, M.A.; Garza-Navarro, M.A.; Gonzalez-Gonzalez, V.A.; Torres-Castro, A.; De La Rosa, J.R. Magnetic nanofibrous materials based on CMC/PVA polymeric blends. *Carbohydr. Polym.* **2018**, *200*, 289–296. [CrossRef]
41. Angel, N.; Guo, L.; Yan, F.; Wang, H.; Kong, L. Effect of processing parameters on the electrospinning of cellulose acetate studied by response surface methodology. *J. Agric. Food Res.* **2020**, *2*, 100015. [CrossRef]
42. Bakar, S.S.S.; Fong, K.C.; Eleyas, A.; Nazeri, M.F.M. Effect of Voltage and Flow Rate Electrospinning Parameters on Polyacrylonitrile Electrospun Fibers. *IOP Conf. Ser.Mater. Sci. Eng.* **2018**, *318*, 012076. [CrossRef]
43. Liu, W.; Wang, D.; Soomro, R.A.; Fu, F.; Qiao, N.; Yu, Y.; Wang, R.; Xu, B. Ceramic supported attapulgite-graphene oxide composite membrane for efficient removal of heavy metal contamination. *J. Membr. Sci.* **2019**, *591*, 117323. [CrossRef]
44. Elessawy, N.A.; Gouda, M.H.; Elnouby, M.; Ali, S.M.; Salerno, M.; Youssef, M.E. Sustainable Microbial and Heavy Metal Reduction in Water Purification Systems Based on PVA/IC Nanofiber Membrane Doped with PANI/GO. *Polymers* **2022**, *14*, 1558. [CrossRef]

45. Hezarjaribi, M.; Bakeri, G.; Sillanpaa, M.; Chaichi, M.J.; Akbari, S.; Rahimpour, A. Novel adsorptive PVC nanofibrous/thiol-functionalized TNT composite UF membranes for effective dynamic removal of heavy metal ions. *J. Environ. Manag.* **2021**, *284*, 111996. [CrossRef]
46. Wang, H.; Xu, H.; Li, H.; Liu, X.; Du, Z.; Yu, W. Electrospun Polyurethane/Zeolitic Imidazolate Framework Nanofibrous Membrane with Superior Stability for Filtering Performance. *ACS Appl. Polym. Mater.* **2020**, *3*, 710–719. [CrossRef]
47. Zhang, X.; Jin, P.; Xu, D.; Zheng, J.; Zhan, Z.-M.; Gao, Q.; Yuan, S.; Xu, Z.-L.; Van der Bruggen, B. Triethanolamine modification produces ultra-permeable nanofiltration membrane with enhanced removal efficiency of heavy metal ions. *J. Membr. Sci.* **2022**, *644*, 120127. [CrossRef]
48. Abdulkarem, E.; Ibrahim, Y.; Kumar, M.; Arafat, H.A.; Naddeo, V.; Banat, F.; Hasan, S.W. Polyvinylidene fluoride (PVDF)-α-zirconium phosphate (α-ZrP) nanoparticles based mixed matrix membranes for removal of heavy metal ions. *Chemosphere* **2021**, *267*, 128896. [CrossRef]
49. Pei, X.; Gan, L.; Tong, Z.; Gao, H.; Meng, S.; Zhang, W.; Wang, P.; Chen, Y. Robust cellulose-based composite adsorption membrane for heavy metal removal. *J. Hazard. Mater.* **2021**, *406*, 124746. [CrossRef]
50. Kamari, S.; Shahbazi, A. High–performance nanofiltration membrane blended by Fe_3O_4@SiO_2–CS bionanocomposite for efficient simultaneous rejection of salts/heavy metals ions/dyes with high permeability, retention increase and fouling decline. *Chem. Eng. J.* **2021**, *417*, 127930. [CrossRef]